Semiannual Progress Report

Project Title:

Optimization of the Cathode Long-Term Stability in Molten Carbonate Fuel Cells: Experimental Study and Mathematical Modeling

PARTICIPANT NAME AND ADDRESS

Dr. Ralph E. White, Project Manager
Department of Chemical Engineering, University of South Carolina
Columbia, South Carolina 29208

Submitted to

Ms. Jo Ann Zysk, Contract Specialist
U.S. Department of Energy
National Energy Technology Laboratory
AAD Document Control, MS 921-107
P.O. Box 10940
Pittsburgh, PA 12236-06940

START DATE October 1, 1999; COMPLETION DATE September 30, 2002

REPORTING PERIOD: April 1st 2000 – September 30th 2000

Abstract

The dissolution of NiO cathodes during cell operation is a limiting factor to the successful commercialization of molten carbonate fuel cells (MCFCs). Microencapsulation of the NiO cathode has been adopted as a surface modification technique to increase the stability of NiO cathodes in the carbonate melt. The material used for surface modification should possess thermodynamic stability in the molten carbonate and also should be electro catalytically active for MCFC reactions. A simple first principles model was developed to understand the influence of exchange current density and conductivity of the electrode material on the polarization of MCFC cathodes. The model predictions suggest that cobalt can be used to improve the corrosion resistance of NiO cathode without affecting its performance. Cobalt was deposited on NiO cathode by electroless deposition. The morphology and thermal oxidation behavior of Co coated NiO was studied using scanning electron microscopy and thermal gravimetric analysis respectively. The electrochemical performance of cobalt encapsulated NiO cathodes were investigated with open circuit potential measurement and current-potential polarization studies. These results were compared to that of bare NiO. The electrochemical oxidation behavior of cobalt-coated electrodes is similar to that of the bare NiO cathode. Dissolution of nickel into the molten carbonate melt was less in case of cobalt encapsulated nickel cathodes. Co coated on the surface prevents the dissolution of Ni in the melt and thereby stabilizes the cathode. Finally, cobalt coated nickel shows similar polarization characteristics as nickel oxide. A similar surface modification technique has been used to improve the performance of the SS304 current collectors used in MCFC cells. SS 304 was encapsulated with nanostructured layers of NiCo and NiMo by electroless deposition. The corrosion behavior of bare and surface modified SS 304 in molten carbonate under cathode gas atmosphere was investigated with cyclic voltammetry, open circuit potential studies, Tafel polarization, impedance analysis and atomic absorption spectroscopy. This study confirms that the presence of surface modification leads to the formation of complex scales with better barrier properties and electronic conductivity.

Introduction

The Molten Carbonate Fuel cell (MCFC), operating at a temperature of 650°C, has been under intensive development for the last few decades as a second-generation fuel cell [1,2]. Significant advances have been done in addressing design issues resulting in the development of prototype MCFC power generators. However, several hurdles remain before commercialization of molten carbonate fuel cells can be realized. The primary challenge remains in the proper selection of materials for the cathode and current collector. Current state-of-art [3] relies on NiO cathodes fabricated from Ni powder. However, during cell operation, nickel oxide dissolves in the electrolyte [4] and does not satisfy long-term stability criteria (over 40,000 hours of operation [5] without replacement). Nickel oxide reacts with CO_2 present in the electrolyte according to an acidic dissolution mechanism.

$$NiO + CO_2 \rightarrow Ni^{2+} + CO_3^{2-}$$

The dissolved nickel remains in equilibrium with the NiO cathode. Simultaneously, the Ni^{2+} cation diffuses to the anode side of the electrolyte and is then reduced in the hydrogen atmosphere to metallic nickel. The diffusion of Ni^{2+} cation fuels more dissolution of nickel from the cathode. Continued deposition of Ni in the anode region eventually leads to a short circuit between the anode and cathode. The dissolution is accelerated under higher CO_2 partial pressure and results in lowering the operating life of the cell. Apart from this, cathode dissolution results in loss of active material and in decrease of the active surface area available for the oxygen reduction reaction (cathodic reaction) leading to degradation in fuel cell performance.

Current state-of-art on solving the Ni dissolution problem is focused on varying the molten salt constituents [6,7] or using alternate cathode materials [8-10]. More basic molten carbonate melts such as Li/Na carbonate eutectic have been used to decrease the Ni dissolution rate in the melt [6,7]. Alkaline earth metal salts based on Ba or Sr have also been used as additives to increase the basicity of the melt. However, using more basic molten carbonate melts only partially solves the problem, since these melts decrease the NiO dissolution rate by 10 to 15% only [6,7].

The other approach to counter the nickel dissolution problem is to either modify NiO or to identify alternate cathode materials, which have longer life in the melt. Alternate electrodes should have good electronic conductivity, chemical stability and proper microstructure for use as

MCFC cathodes. $LiFeO_2$ and $LiCoO_2$ offered initial promise as replacement material for NiO cathodes [8-10]. However, the exchange current density for oxygen reduction reaction on $LiFeO_2$ is about two orders of magnitude lower than that on NiO. Thus, the slow kinetics for oxygen reduction limits the possibilities for further improvement of cathodes based on this material. $LiCoO_2$ is more stable than NiO in alkaline environment [8]. However, $LiCoO_2$ is less electronically conductive than NiO and is more expensive than NiO. Other choices for cathode materials have failed on either one of these factors namely – low electronic conductivity and poor oxygen reduction kinetics. This being the case, surface modification of NiO with more resistant materials is being considered as the more viable alternative.

Based on previous investigations [11,12] cobalt has been chosen to modify the surface of the NiO cathode and reduce its dissolution. Fukui *et al* [11] and Zhang *et al* [12] studied the effect of cobalt coating on nickel oxide particles used as cathodes in MCFCs. Ni particles were covered with CoO particles mechanically. Composites made of the Ni-CoO particles showed better corrosion resistance as compared to that of conventional NiO in Li-K carbonate melt. However, polarization characteristics of the Ni-CoO composite were not shown. Materials chosen for modifying the NiO surface should not affect the performance of the MCFC cathode. A simple first principles model was developed to understand the influence of exchange current density and conductivity of the electrode material on the polarization of MCFC cathodes. The model predictions suggest that cobalt can be used to improve the corrosion resistance of NiO cathode without affecting its performance.

Hence the objective of this study is to synthesize and characterize Co coated NiO as a cathode material in molten carbonate fuel cells. The first goal is to synthesize NiO cathode encapsulated with cobalt. Next, the electrochemical polarization behavior of cobalt coated nickel oxide electrodes will be studied. Finally, material characterization will be done to ascertain changes in the NiO morphology and surface due to cobalt encapsulation. The second part of this study is focussed on using the surface modification technique to improve the performance of the SS304 current collectors used in MCFC cells. The corrosion behavior of stainless steel components in molten carbonate conditions has been studied extensively during the past decade. The corrosion resistance of stainless steels and nickel-base alloys in aqueous solutions can often be increased by addition of chromium or aluminum. Previous studies done to characterize the corrosion behavior of chromium in MCFC conditions have shown the formation of several

lithium chromium oxides by reaction with the electrolyte. This corrosion process also results in increased ohmic loss due to formation of scales on the steel. Aluminum additions similarly have a positive effect on corrosion resistance. Electroless plating of Ni-Co gives rise to deposition of uniform layers of nanostructured material, which would result in better protection of the substrate. The objective of this work is therefore to synthesize electroless Ni-Co over SS 304 substrate and characterize it in MCFC cathode conditions. The corrosion characteristics of both SS 304 and surface modified SS 304 have been studied using a variety of electrochemical and surface characterization techniques.

Experimental

Tape casting: - Porous nickel cathode was made by a tape casting and sintering process. Nickel (Aldrich company) particles were ground and sieved to obtain uniform particles of size 3-5 μm. The tape casting slurry was prepared by ball milling nickel powder in water with suitable binder (PVA) and plasticizer (glycerol). The ball milling was done in two steps. At the first step, 50 g of nickel powder were added to 5 g of PVA (PVA liquid 15 wt.%) and 1 g of defoamer (Airdefoam™ 60, Air Products). The ingredients were mixed thoroughly with 15 g of water and the slurry was ball milled for 3 hr in order to break the weak agglomerates. Next, 9 g of glycerol was added to the above suspension and the resulting slurry was ball milled for an additional 3 hr. The slurry was then slightly warmed (50° C) and degassed using a ROTOVAP® evaporator. The slurry was cooled and then cast using a doctor blade assembly over a glass plate coated with silicone oil. The drying was performed slowly at room temperature for about 48 hours. The cast plate nickel tape is then stripped off gently from the glass plate and stored.

Sintering: - Sintering of the tape casted electrodes influences the cathode pore structure and thereby affects its electrochemical performance. TGA was done to determine the optimum heat treatment schedule for sintering. A typical TGA curve for green nickel tape is shown in Figure 1. The as cast Ni tape is pre-heated at 120°C for 12 hours in order to remove all the crystalline water in the tape. TGA analysis was done by heating the sample from 100°C to 650°C at a rate of 10°C/min. A steep reduction in weight (15 wt%) is seen on heating the sample to 200°C due to the removal of the binder. A secondary weight loss (5 wt%) is noticed between 300°C to 400^{o} C due to the removal of plasticizer. The removal of all volatile and decomposable organic matter is completed below 400°C. On heating the sample above 400^{o} C oxidation of nickel surface takes

place. The total weight loss varies between 15 to 20 wt % depending upon the binder and plasticizer contents in the green tapes. Since, Ni is oxidized beyond 400^{o} C, it is critical to heat the sample in a reducing atmosphere to prevent oxidation during sintering. Further, the rate of heating should be very slow initially to ensure complete burn out of binder and plasticizer. Based on the above TGA analysis, we chose the following heating pattern to be followed for sintering of the electrodes.

Green tapes were cut out to specific area (10 cm x 10 cm) and were placed between two porous alumina plates inside a programmable tube furnace. The heating schedule consists of the following stages: (i) first, start from room temperature and heat to 130°C at a rate of 1°C/min in nitrogen atmosphere, (ii) hold the temperature at 130°C for 10 hours, (iii) next, raise the temperature to 230°C at a rate of 1°C/min in nitrogen atmosphere, (iv) hold the temperature at 230°C for 2 hours, (v) raise the temperature to 400°C at 1°C/min in nitrogen atmosphere, (vi) hold the temperature at 400°C for 2 hours, (vii) finally, raise the temperature to 800°C at 1°C/min in hydrogen atmosphere, (viii) hold the temperature at 800°C for 1 hour and (ix) cool to room temperature at 1°C/min in hydrogen atmosphere.

Cobalt Coating: - Cobalt encapsulation on nickel tapes was carried out using a procedure developed in our laboratories. The procedure has been described previously [13]. The cobalt encapsulated nickel tape was rinsed with deionized water, dried at 65°C for 4 hours and later sintered at 800°C in hydrogen atmosphere for 2 hours.

After cobalt encapsulation, the samples were directly taken from room temperature to 800°C at 10°C/min and were kept at 800°C for two hours before cooling it back at 1°C/min. The entire heating and cooling procedure was done in a hydrogen atmosphere. This was done to remove all decomposable material, which could have been incorporated into the Ni laminate during Co deposition.

Pot cell studies: - In order to determine the solubility of nickel and cobalt encapsulated nickel electrodes in molten carbonate, pot tests were carried out under cathode gas conditions. Pellet electrodes of 2.5 cm dia were cut out from sintered nickel and cobalt encapsulated nickel tapes. They were weighed and carefully dropped inside an alumina crucible containing 100 g of molten carbonate (Li_2CO_3/K_2CO_3=62/38) at 650°C. Cathode gas (30% CO_2/70% air) was bubbled through the carbonate melt using alumina tubes. About 0.2 g of molten carbonate was taken from

the melt approximately every 6 hours upto 200 hours using an alumina rod. The molten carbonate sample was dissolved in 10% dilute acetic acid. Atomic absorption spectroscopy was used to analyze the concentration of dissolved nickel and cobalt.

Electrochemical Characterization of Cathode: In-situ oxidation of nickel and cobalt encapsulated nickel electrodes were studied using a three-electrode half-cell shown in Figure 2a. The working electrode was made of circular disc electrodes cut from sintered metal tapes and spot welded with a gold wire. Gold was used as the counter electrode and $Au/(2CO_2+1O_2)$ served as the reference electrode. The reference gas flow rate was maintained at 10 cc/min. Oxidant gas with a composition of 30% CO_2 and 70% air (National Welders) was directly purged into the carbonate melt through an alumina tube. The open circuit potential studies were done using an EG&G PAR model 273 potentiostat interfaced with a computer.

Fuel cell performance studies were done in a 3-cm^2-lab cell shown in Figure 2b. Nickel and cobalt-encapsulated nickel were used as the cathode while Ni-Cr served as the anode. $(Li_{0.62}K_{0.38})_2CO_3$ eutectic embedded in a $LiAlO_2$ matrix was used as the electrolyte. Oxidant and fuel gas compositions were 70% air/30% CO_2 and 80% H_2/20%CO_2 respectively. Two oxygen reference electrodes ($Au/CO_2/O_2$) connected to the electrolyte tile with a salt bridge ($50\%(Li_{0.62}K_{0.38})_2CO_3$ + $50\%LiAlO_2$) were used to monitor the polarization of cathode and anode. Current-voltage characteristics were obtained by varying the current load on the cell.

Scanning Electron Microscope (SEM) was used to study the microstructure of the specimens. Thermal Gravimetric Analysis (TGA) was employed to investigate the thermal oxidation behavior of both cobalt encapsulated and bare nickel electrodes in the presence of cathode gas conditions. The oxidation behavior was studied both in the presence and absence of the carbonate melt.

Current Collector Studies: Electrodes of area 1 cm^2 were made from a perforated stainless steel 304 (Perforated Metals Inc.), with a void area of 45%. Gold wires were spot welded to the flat electrodes to serve as a current collector during electrochemical studies. The electrodes were cleaned with alkali and were washed in distilled water before the characterization studies in order to be free of any contaminants. Ni-Co encapsulation on SS 304 electrodes was carried out using a procedure developed in our laboratories. In-situ oxidation of bare and surface modified SS 304 electrodes were studied using a three-electrode half-cell shown in Figure 2. Square electrodes (1 cm x 1 cm) cut from bare and surface modified SS 304 were spot welded with a gold wire and

was used as the working electrode. Gold was used as the counter electrode and Au/($2CO_2$+$1O_2$) served as the reference electrode. The reference gas flow rate was maintained at 10 cc/min. Oxidant gas with a composition of 30% CO_2 and 70% air (National Welders) was directly purged into the $(Li_{0.62}K_{0.38})_2CO_3$ eutectic melt through an alumina tube. The open circuit potential studies were done using an EG&G PAR model 273 potentiostat interfaced with a computer.

Model Development

The standard model for porous electrodes in MCFC has been the agglomerate model. This model assumes that the porous electrode has two distinct pore sizes. The micropores in the agglomerate are assumed to be flooded with electrolyte while the macropores are assumed to contain only gas. Using this model Lee *et al.* [14] compared the performance of different cathode materials. Prins-Jansen *et al.* [15] have modified the agglomerate model by neglecting that the gas and electrolyte phases are present in separate pores. Instead they assume that all three phases co-exist within the porous electrode. Using this approach the microscopic equations have been averaged over the entire electrode to derive homogenized macroscale equations. The validity of this model was proved by comparing it to ac-impedance spectra recorded from MCFC cathodes. Our present approach is based on Newman and Tobias [16] and considers all three phases to be present in the electrode agglomerate.

We define a potential in the electrolyte pore as Φ^1, and another in the solid phase as Φ^2. Corresponding to these we have two different current densities, i^1 that refers to the current in the liquid phase and i^2, which refers to current in the solid phase. If we assume that the concentration of active species remains constant in the electrolyte pore, the ionic current density is given by,

$$i^l = -\kappa \nabla \Phi^1 \qquad [1]$$

where κ is the liquid phase conductivity. For the matrix Ohm's law applies,

$$i^2 = -\sigma \nabla \Phi^2 \qquad [2]$$

where σ is the solid phase conductivity. Based on conservation of electroneutrality we know that the sum of the electronic current density and ionic current density equals the overall applied current density, I_T. Hence,

$$\nabla i^l + \nabla i^2 = 0 \qquad [3]$$

Finally, the transfer of current from the solid phase to the liquid phase is given by,

$$\nabla i^{l} = \frac{a}{F} \sum_{j=1}^{j=NR} \frac{i_j}{z_i} \qquad [4]$$

where the local reaction rate, i_j, is given by

$$i_j = i_{oj,ref} \left\{ \begin{array}{l} \prod_i \left(\frac{c_i}{c_i^o} \right) \exp\left[\frac{\alpha_{aj} F}{RT} \left(\Phi^2 - \Phi^1 - \Phi_j^o \right) \right] - \\ \prod_i \left(\frac{c_i}{c_i^o} \right) \exp\left[\frac{-\alpha_{cj} F}{RT} \left(\Phi^2 - \Phi^1 - \Phi_j^o \right) \right] \end{array} \right\} \qquad [5]$$

The boundary conditions are given by:

At matrix	At current collector
$i^1 = I_{total}$	$i^1 = 0$
$i^2 = 0$	$i^2 = I_{total}$
$\nabla\Phi^1 = \frac{-I_{total}}{\kappa}$	$\nabla\Phi^1 = 0$
$\nabla\Phi^2 = 0$	$\nabla\Phi^2 = \frac{-I_{total}}{\sigma}$

[6]

The above set of conditions has been solved using Newman's Band(J**)** [17]. Table 1 summarizes the parameters used for the simulation.

Results and Discussion

Model Simulations:- Figure 3 shows model predictions on the polarization characteristics of different molten carbonate cathode materials. For a porous electrode various factors such as activation resistance, ohmic resistance and electrolyte conductivity affect the polarization behavior of the cathode. The model has been used to analyze the role of these different parameters in influencing the electrode behavior. In this case, the poor performance of lithiated iron oxide arises due to its low electronic conductivity and exchange current density. Among all three electrodes nickel oxide exhibits the best ohmic conductivity and reaction kinetics. This reflects in the very low polarization of the cathodes made of NiO as seen from Figure 3. The cathode polarization results shown in Figure 3 agree with the previous theoretical and experimental investigations of Lee *et al* [14] and hence confirm the validity of the model.

Next the model was used to predict the influence of electrode conductivity on cathode polarization. Figure 4 shows the cathode polarization obtained for different conductivities at a

constant applied load of 160 mA/cm^2. As seen from the plot, change in conductivity significantly affects the performance of cathodes. An electrode made of a material, which has the exchange current density of NiO, and conductivity of $LiCoO_2$ would suffer 7% more polarization than the conventional NiO cathode for the same load. *In-situ* oxidized and lithiated NiO ($Li_xNi_{1-x}O$) has a low lithium content ($0.02 < x < 0.05$). NiO is a p type semiconductor and has a lower conductivity than pure Ni. Li^+ ions coming from the electrolyte, diffuse into the NiO and increase its electronic conductivity. Cobalt oxide is also a p-type semiconductor like NiO. The ionic conduction in CoO is primarily due to the movement of holes and behaves entirely different from $LiCoO_2$. Surface modification of Ni cathodes with Co would result in the diffusion of Li^+ ions into Co during the lithiation process. $Li_xCo_{1-x}O$ (x=2 to 5 mol%) possesses conductivity values, which are very similar to that of lithiated NiO with similar amounts of Li [18]. Therefore, the polarization performance in case of Co coated Ni cathodes can be assumed to be similar to that of NiO.

Figure 5 shows the dependence of cathode polarization on the exchange current density for oxygen reduction. The curve has been generated assuming a constant conductivity (equal to that of NiO) and an applied load of 160 mA/cm^2. The dependence of cathode polarization on oxygen reduction kinetics is more pronounced than its dependence on electrode conductivity. An electrode made of a material, which has the conductivity of NiO, and exchange current density of $LiCoO_2$ would suffer around 50% more polarization than the conventional NiO cathode. Similarly, cathodes made of $LiFeO_2$ have polarization losses five times higher than that of NiO. Thus reaction kinetics plays a very important role in material selection. Availability of kinetic data regarding oxygen reduction on cobalt is very limited. However, considering the performance of $LiCoO_2$, one can expect *in-situ* lithiated CoO to perform similar to (if not better than) $LiCoO_2$. Thus the basis for choosing cobalt as a coatant material to decrease the dissolution is partly justified. The next section deals with the morphology and stability studies done on cobalt encapsulated and bare NiO cathodes.

Scanning Electron Micrograph: - Figure 6 shows the SEM images of Ni and cobalt encapsulated nickel electrodes prepared by the above sintering procedure. The sintered matrix shown in Figure 6 has the same pore structure before and after Co coating. The primary particle size for nickel electrodes was in the range of 0.5 – 4 μm. Subsequent to Co encapsulation the particles tend to

agglomerate together. The morphological difference between nickel and cobalt-encapsulated nickel can be attributed to the cobalt deposited over the nickel surface and the additional sintering done on the sample.

Stability tests: - The short-term stability of cobalt encapsulated and bare nickel in molten carbonate eutectic were determined using pot tests. Atomic absorption (AA) was used to analyze the dissolved nickel and cobalt in the melt. Figure 7 shows the results of AA analysis on the amount of dissolved nickel and cobalt in the carbonate melt as a function of time. As shown in the plot, the solubility of Ni^{2+} was more than two times higher in case of bare nickel when compared to that of cobalt microencapsulated nickel. Solubility of cobalt was about one order of magnitude lesser than that of nickel. The results indicate that cobalt is more resistive to the molten carbonate environment. The amount of nickel and cobalt cations in the carbonate melt increases with time and saturates after about 100 hours. Similar results have been obtained in the literature for the solubility of Ni^{2+} and Co^{2+} ions in the carbonate melt [19-23]. Based on our data and prior results we can conclude that cobalt coating will decrease the dissolution of nickel in the melt.

Thermal oxidation behavior: - In order to study the performance of the sintered electrodes under cathode gas conditions, TGA was done on the sintered nickel and cobalt encapsulated nickel tapes. The temperature was increased from 100°C to 650°C at a rate of 10°C/min under cathode gas atmosphere (30% CO_2+70% air). The temperature was then maintained at 650°C for a period of two hours. Figure 8a shows the results of TGA analysis obtained for nickel tapes in the presence and absence of molten carbonate. The percentage increase in weight while heating the sample is plotted against the experiment time. The time interval between 0 and 55 minutes corresponds to a temperature rise from 100°C to 650°C at a heating rate of 10°C/min. The time interval after 55 min corresponds to the period where the temperature was maintained constant at 650°C. As shown in Fig. 8, the weight of nickel sample in the absence of molten carbonate starts to increase after 40 min corresponding to a temperature of 400°C and stabilizes after about 2 hours at 650°C. On the other hand, the oxidation of nickel was rapid in case of nickel sample placed with molten carbonate salt in the presence of cathode gas. It appears that O_2 permeation and reaction with inner nickel particles is enhanced in the presence of molten carbonate. The weight increase in both the cases was about 27%, which suggests the complete conversion of Ni to NiO.

Oxidation of cobalt-coated nickel was very slow in the absence of molten carbonate and the oxidation continued even after two hours after reaching 650°C as shown in Figure 8b. Theoretical weight increase for the conversion of Ni and Co to their oxides (NiO/CoO) based on stochiometric calculation is around 27%. In the presence of molten carbonate, weight of the cobalt encapsulated substrate continued to increase due to oxidation and stabilized shortly after reaching 650°C. The percentage increase in weight was around 22 %. However, the actual weight increase is much lower in the absence of the carbonate melt (60 % lower than with the presence of molten carbonate). This slow oxidation of cobalt encapsulated nickel specimen is obviously due to the presence of cobalt, which is thermodynamically more stable.

Electrochemical oxidation behavior: - To understand the influence of cobalt encapsulation on nickel electrode from an electrochemical point of view, the open-circuit potentials of both samples were monitored as a function of time during the *in-situ* oxidation process. The oxidation was carried out in a three-electrode half-cell described in the experimental section (Figure 2). Oxidant gas composition of 67% CO_2 and 33% O_2 was bubbled at a constant rate of 60 cc/min through an alumina tube during the *in-situ* oxidation process. Figure 9 compares the OCP behavior of bare and cobalt encapsulated nickel electrodes as a function of immersion time.

In both cases, three different potential plateaus are observed. Nickel oxidation in MCFC has been studied extensively and the observed plateaus have been attributed to the following reactions [8, 9]

$$Ni + CO_3^{2-} \rightarrow NiO + CO_2 + 2e^- \qquad \text{-0.80 V}$$

$$2Ni + 3CO_3^{2-} \rightarrow Ni_2CO_3 + 3CO_2 + 2e^- \qquad \text{-0.43 V}$$

$$Ni + CO_3^{2-} \rightarrow NiCO_3 + 2e^- \qquad \text{-0.25 V}$$

The first plateau in case of nickel oxidation is due to the formation of porous nickel oxide on the surface of the nickel matrix. Next, bulk nickel is oxidized to NiO at approximately –0.6 V. The second plateau at –0.44 V has been attributed to the surface oxidation of Ni(II) oxide to trivalent nickel.

The redox processes that occur during the *in-situ* oxidation of cobalt are given [9, 10].

$$Co + CO_3^{2-} \rightarrow CoO + CO_2 + 2e^- \qquad \text{-0.85 V}$$

$$2Co + 4CO_3^{2-} \rightarrow Co_3O_4 + 4CO_2 + 8e^- \qquad \text{-0.68 V}$$

$$Co + CO_3^{2-} \rightarrow CoCO_3 + 2e^- \qquad \text{-0.35 V}$$

In the case of Co coated Ni, we can expect the OCP behavior to represent a mixed potential due to oxidation of both surface Co and Ni.

Polarization studies: -Polarization studies were carried out in a 3 cm^2 lab scale cell containing nickel/cobalt encapsulated nickel electrode as the cathode and Ni-Cr (9:1) as the anode. The electrodes were separated by a $LiAlO_2$ ceramic tile containing Li/K carbonate melt (62-38). The cells are connected to an oxygen reference electrode through a salt bridge. The working electrode (cathode) potential is monitored with respect to the reference electrode. The i-V characteristics of 3 cm^2 lab cells were obtained by varying the cell current load. Figure 10 compares the cathode polarization as a function of current density (mA/cm^2) for the two cathode materials. The i-V characteristics (Fig. 10) of both NiO and Co coated NiO are similar to each other. Increasing the applied current results in an increased polarization. The Co encapsulated cathode has a slightly larger potential drop as compared to the bare NiO electrode. Since the experiments have been done under similar conditions, the difference can be attributed to a lower oxygen reduction rate on the cobalt-coated cathode. Since, we have coated the Ni electrode with Co, we can expect a small drop in the reaction rate. Hence, the cathode polarization plots show a slightly higher polarization in case of cobalt-microencapsulated electrodes. The polarization losses in case of $LiCoO_2$ is about 60% higher than NiO cathode for an applied load of 160 mA/cm^2. However, cobalt coated nickel oxide has a polarization loss of 33% when compared to that of NiO. This shows that Co coating on NiO cathode performs better than $LiCoO_2$.

EDAX Analysis: - EDAX analysis was carried out to characterize the cobalt content in the cobalt encapsulated cathodes after 72 hours and 300 hours of polarization. EDAX pattern was very identical in both the cases as shown in Figure 11. The concentration calculations based on the intensity peaks show that the cobalt and nickel concentration slightly decreases. This could be due to the completion of oxidation and the corresponding increase in oxygen concentration. Other than this, there was no significant change in the concentrations of cobalt and nickel. Thus cobalt coating offers a viable solution to limit the solubility of nickel oxide in molten carbonate eutectic.

Current Collector Studies - Corrosion Studies Under Open Circuit Conditions: - At open circuit conditions, the potential of bare and surface modified SS 304 changes with increased exposure times from –1 V to the potential of oxygen reduction reaction. This potential change as shown in

Figure 12 is a multi-step process based on the different oxidation reactions happening at the surface. In the potential range of interest namely –1.0 V to 0.0 V, iron gets oxidized to FeO and $LiFeO_2$, nickel to lithiated NiO and trivalent nickel oxide and chromium to $LiCrO_2$ and Li_2CrO_4. The different corrosion reactions and associated products in this potential range were elaborated in the cyclic voltammogram studies.

Surface composition of the alloy strongly determines the nature of the potential change and the time scale at which the changes occur. Growth of a passive layer is a nucleation and growth process. Hence the complexity of this passive layer strongly depends on the surface composition of the alloy. The open circuit profile traced in case of surface modified SS 304 is seen to be different than that of bare SS 304 suggesting the different nature of the corrosion scale.

The first potential shift under cathode gas conditions can be attributed to the surface oxidation of the sample and coverage with a stable layer of mostly oxides of chromium. Chromium oxidizes much faster than iron. The rate of dissolution is also very high in case of chromium when compared to iron oxides. Chromium dissolution into the melt leads to the exposure of underlying iron oxides. These oxides react with the lithium carbonate to form lithium ferrite, which again is not a good barrier to diffusion of chromium. Hence external diffusion of chromium and subsequent dissolution into the melt proceeds thereby coloring the melt. The outer porous lithium ferrite layer however prevents the direct interaction of the inner lithium chromite layer with the molten carbonate. The inner lithium chromite layer also prevents the external diffusion of other metal ions thereby checking the growth of external ferrite layer. This phenomenon is completely dependent on the surface composition of the sample and the composition of the external scale. However, an analysis of the dissolved elements will qualitatively indicate the barrier performance of this corrosion scale.

Tafel polarization Studies on Current Collector: - Cyclic voltammograms indicate higher corrosion in case of bare SS 304 samples. However, some other electrochemical technique has to be used to quantify the surface corrosion under open circuit conditions. To estimate corrosion rates, Tafel extrapolation from potentiodynamic curves were measured between OCP ± 300 mV after different times of exposure. The potential was scanned at a rate of 25 mV/s. Corrware® software (Scribner) was used to obtain the Tafel fit of the potentiodynamic curves. Table 2 presents the open circuit potential and polarization resistance values obtained for bare and

surface modified SS 304 under cathode gas conditions after different times of exposure to molten carbonate melt. The polarization resistance rapidly increases with exposure time signifying the increasing corrosion scale thickness.

Electrochemical impedance spectroscopy: - Oxidation of stainless steel current collector in MCFC cathode conditions is a rapid process and therefore a steady state technique would give better results than the Tafel extrapolation method. However, the high scan rate employed during the Tafel extrapolation method ensures minimal damage to the surface during the time of experiment. EIS studies were done using the model 352 SoftCorr system with EG&G Princeton applied Model 273A potentiostat/galvanostat and a Solartron frequency analyzer. The impedance data generally covered a frequency range of 1 mHz to 100kHz. A sinusoidal ac voltage signal varying by ± 5 mV was applied. Figure 13 shows the Nyquist response of impedance analysis of bare and surface modified SS 304 after different times of exposure to the molten carbonate. R_p values can be approximately determined by fitting the Nyquist response to a simple equivalent circuit consisting of ohmic resistance, double layer capacitance and polarization resistance. Bare SS 304 has R_p values very similar to those obtained using Tafel extrapolation method. The polarization resistance of surface modified SS 304 is considerably smaller than that of bare SS 304. This can be understood to be due to the presence of thinner corrosion scale. The curves shown in Figure 13 are composed of two (in some cases three) overlapping semi-circles. They may again be due to the effect of multi layered corrosion scale and the porosity of these layers. Further, studies are to be done to evaluate these individual depressed semi-circles.

Conclusions

Nickel cathodes for MCFC were made by a tape casting and sintering process. Subsequently, they were treated using a surface modification technique wherein a thin film of cobalt was formed over the sintered tape. SEM analysis on nickel and cobalt encapsulated nickel electrodes show slightly bigger agglomerates in case of cobalt-coated electrodes. Further, cobalt coated electrodes have a lower solubility in the molten carbonate melt when compared to bare nickel electrodes in the presence of cathode gas conditions. The solubility decreased more than 50% due to micro encapsulation with cobalt. The oxidation behavior of cobalt-encapsulated electrode was very similar to that of bare Ni. However, thermal oxidation rate was much lower in case of cobalt-encapsulated electrode. The open circuit potential showed three distinct plateaus

as a function of time with each plateau corresponding to a unique redox process for both electrodes. The i-V characteristics and polarization behavior for both NiO and Co encapsulated NiO are similar to each other. This suggests that cobalt encapsulation can be regarded as an alternative to improve the performance of conventional nickel oxide cathodes in molten carbonate fuel cells.

Surface modification of SS 304 was carried out by electroless plating of monolayers of nanostructured NiCo and NiMo. The open circuit potential response of the surface modified and bare SS 304 was measured as a function of the exposure time. The several plateaus observed in the OCP response implied the different corrosion reactions happening on the surface of the sample. Tafel extrapolation experiments were used to determine the polarization resistance and the trend in corrosion currents indicated a lower corrosion scale thickness in case of surface modified SS 304. Polarization resistance values estimated from complex impedance plots agreed with those obtained using Tafel extrapolation method.

References

[1] A. J. Appleby and F. R. Foulkes, Fuel Cells – Hand Book, Von Nostrand Reinhold, New York (1989).

[2] K. Joon, J. Power Sources, **71** (1998) 12.

[3] J. R. Selman, Assesment of research needs for advanced fuel cells by the DOE advanced fuel cell working group (AFCWG), S.S. Penner, Editor, Permagon Press, New York (1984).

[4] T. G. Benamin, E. L. Camara and L. G. Marianowski, Handbook of Fuel Cell Performance, Contract no. EC-77C-03-1545, Chicago, IL, (1980).

[5] L. Christner, L. Paetsch, P.Patel and M. Farooque, Scale-up of internal reforming molten carbonate fuel cells. Proceedings of the 1988 Fuel Cell Seminar, Long Beach, CA (1988) 403.

[6] K. Tanimoto, Y. Miyazaki, M. Yanagida, S. Tanase, T. Kojima, N. Ohtori, H. Okuyama, T. Kodama, Denki Kagaku, **59**(7) (1991) 619.

[7] K. Tanimoto, Y. Miyazaki, M. Yanagida, T. Kojima, N. Ohtori, T. Kodama, Denki Kagaku, **63**(4) (1995) 316.

[8] L. Plomp, E.F. Sitters, C. Vessies, F. C. Eckes, J. Electrochem. Soc., **138**(2) (1991) 629.

[9] L. Giorgi, M. Carewska, S. Scaccia, E. Simonetti, F. Zarzana, Denki Kagaku, **64**(6) (1996) 482.

[10] C. Lagergren, A. Lundblad, B. Bergman, J. Electrochem. Soc., **141**(11) (1994) 2959.

[11] T. Fukui, S. Ohara, H. Okawa, T. Hotta, M. Naito, J. Power Sources, **86** (2000) 340.

[12] X. Zhang, H. Okawa, T. Fukui, Denki Kagaku, **66**(11) (1998) 1141.

[13] A. Durairajan, B. Haran, B. Popov and R. White, J. Power Sources, **83** (1999) 114.

[14] G. L. Lee, J. R. Selman and L. Pomp, **140** (1993) 390.

[15] J. A. Prins-Jansen, J. D. Fehribach, K. Hemmes, and J. H. W. de Wit, J. Electrochem. Soc., **143** (1996) 1617.

[16] J. Newman and C. W. Tobias, **109** (1962) 1183.

[17] J. S. Newman, Electrochemical Systems, 2nd Ed., Prentice-Hall, New Jersey, 1991.

[18] Lange F, Martin M, Beriche Der Bunsen-Gesellschaft –Physical Chemistry Chemical Physics, **101** (2) (1997) 176.

[19] K. Tanimoto, Y. Miyazaki, M. Yanagida, S. Tanase, T. Kojima, N. Ohtori, H. Okuyama, T. Kodama, Denki Kagaku, **59**(7) (1991) 619.

[20] K. Ota, S. Mitsushima, S. Katao, S. Asano, H. Yoshitake, and N. Kamiya, J. Electrochem. Soc., **139**(3) (1992) 667.

[21] X. Zhang, P. Capobianco, A. Torazza, and B. Passalacqua, Electrochemistry, **67**(6) (1999).

[22] J. B. J. Veldhuis, F. C. Eckes, and L. Plomp, J. Electrochem. Soc., **139** (1) (1992) L6.

[23] K. Ota, Y. Takeishi, S. Shibata, H. Yoshitake, and N. Kamiya, J. Electrochem. Soc., **142**(10) (1995) 3322.

List of Figures

potential is referenced to the oxygen reduction reaction happening on a gold electrode.

Figure 13. Nyquist plots of bare and surface modified SS 304 recorded after 1 hour and 10 days after immersion in molten carbonate melt under cathode gas conditions.

Table 1a. List of parameters used for the simulation of cathode polarization curves (common to all the cathodes studied)

Parameter, Symbol	Value
Thickness of the cell, L	0.08 cm
Universal gas constant, R	8.314 J/K/mol
Faraday's constant, F	96487 J/C
Anodic transfer coefficient, α_a	0.5
Anodic transfer coefficient, α_c	0.5
Electrolyte phase conductivity, d_κ	1.386 S/cm

Table 1b. List of parameters used for the simulation of cathode polarization curves

Parameter	Ni	Co	$LiFeO_2$	Ref.
Solid phase conductivity, σ	13 S/cm	0.61 S/cm	0.1 S/cm	14
Exchange current density, $i_{o,ref}$	0.81×10^{-3} A/cm^2	0.50×10^{-3} A/cm^2	0.10×10^{-3} A/cm^2	14

Table 2. Polarization resistance (R_p) determined with Tafel extrapolation after different times of exposure in Li/K under cathode gas conditions for bare and modified SS304.

	SS 304		Ni-Mo-P		Ni-Co-P	
Time (h)	OCP	R_p (Ω)	OCP	R_p (Ω)	OCP	R_p(Ω)
1	-0.864	580	-0.842	300	-0.622	400
8	-0.636	820	-0.343	380	-0.436	600
15	-0.025	1400	-0.022	420	-0.026	740
240	-0.006	1800	-0.010	480	-0.013	900

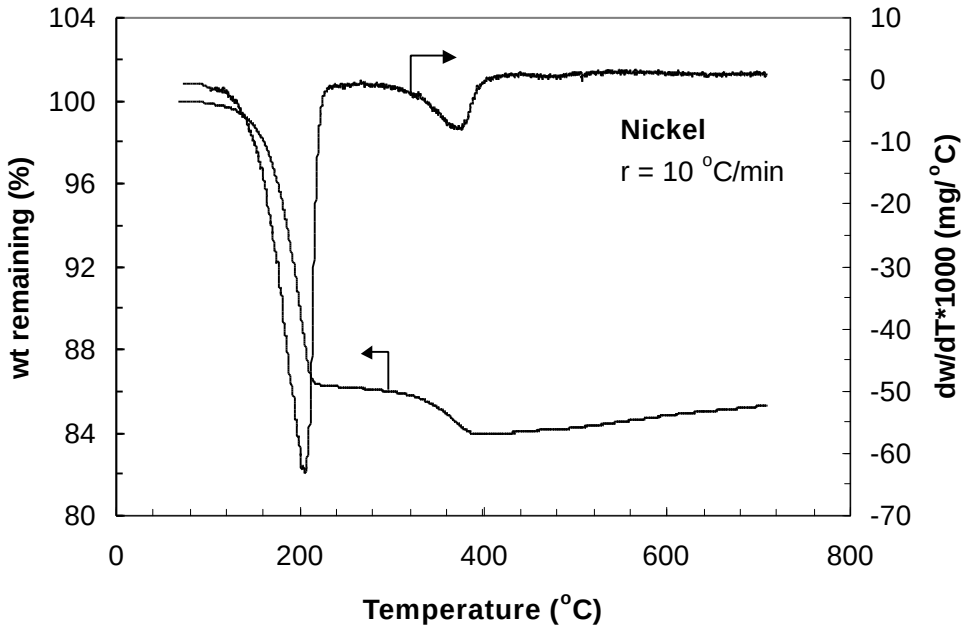

Figure 1. Thermo gravimetric analysis (TGA) of an aqueous nickel tape.

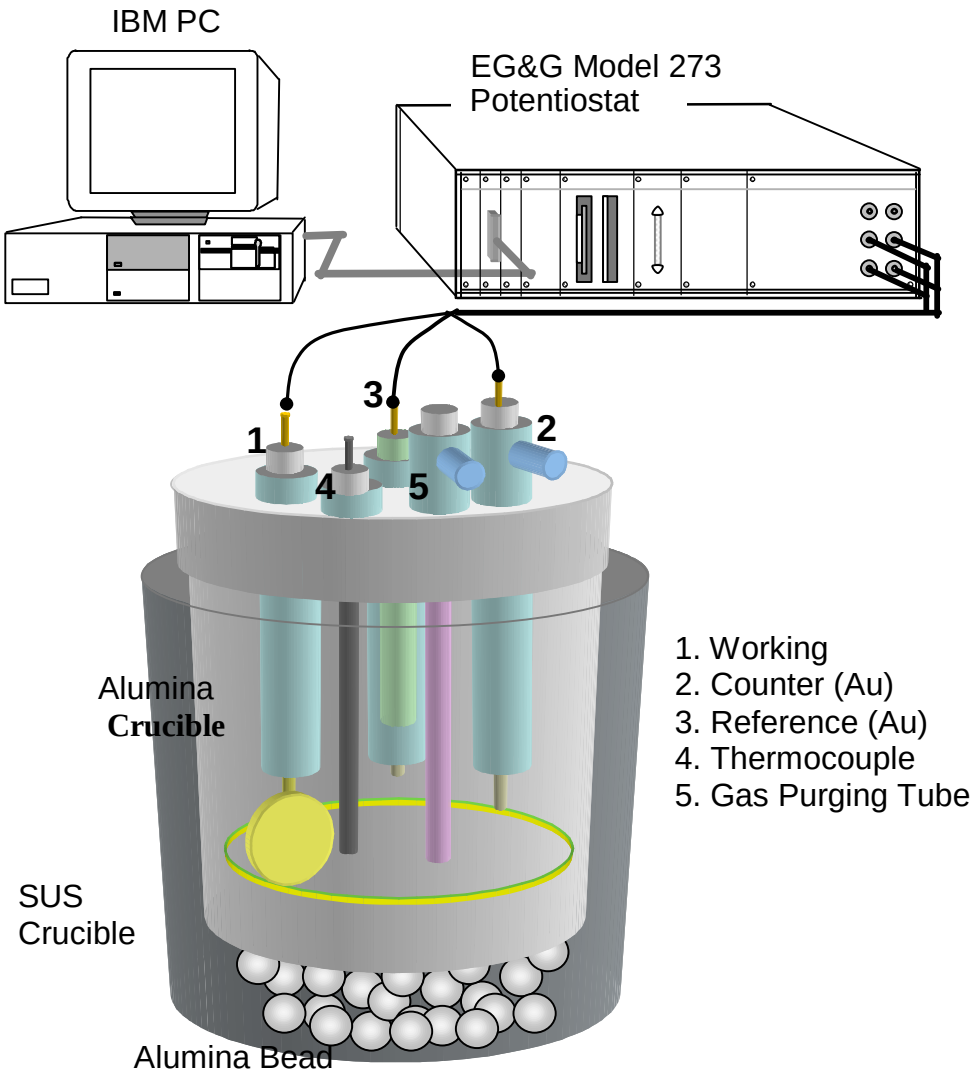

Figure 2a. Schematic diagram of a three-electrode half-cell used for carrying out electrochemical characterization and cathode dissolution studies.

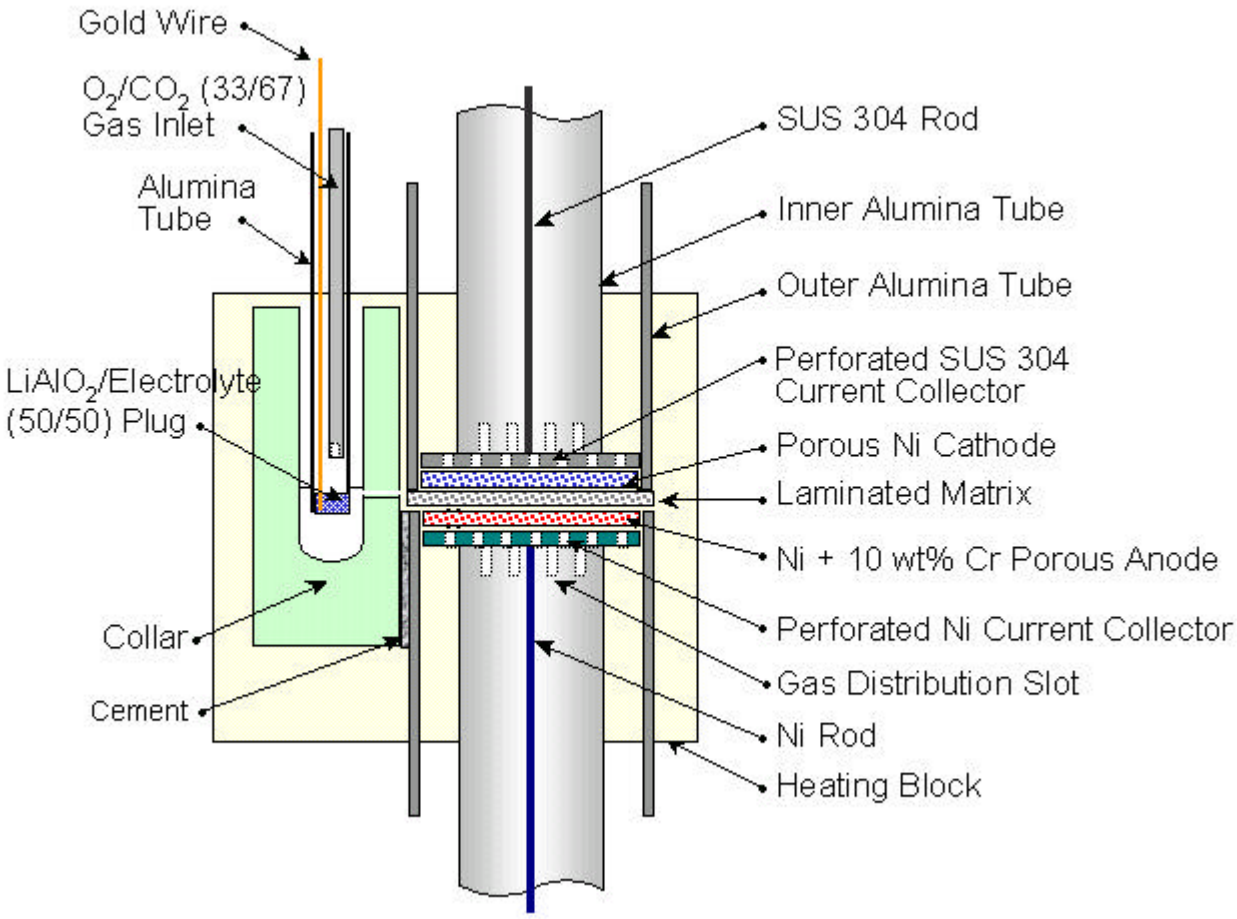

Figure 2b. Schematic diagram of a 3-cm^2-electrochemical fuel cell. Au/($2CO_2$+$1O_2$) reference electrode with a salt bridge was used for measuring cathode and anode potential during polarization studies.

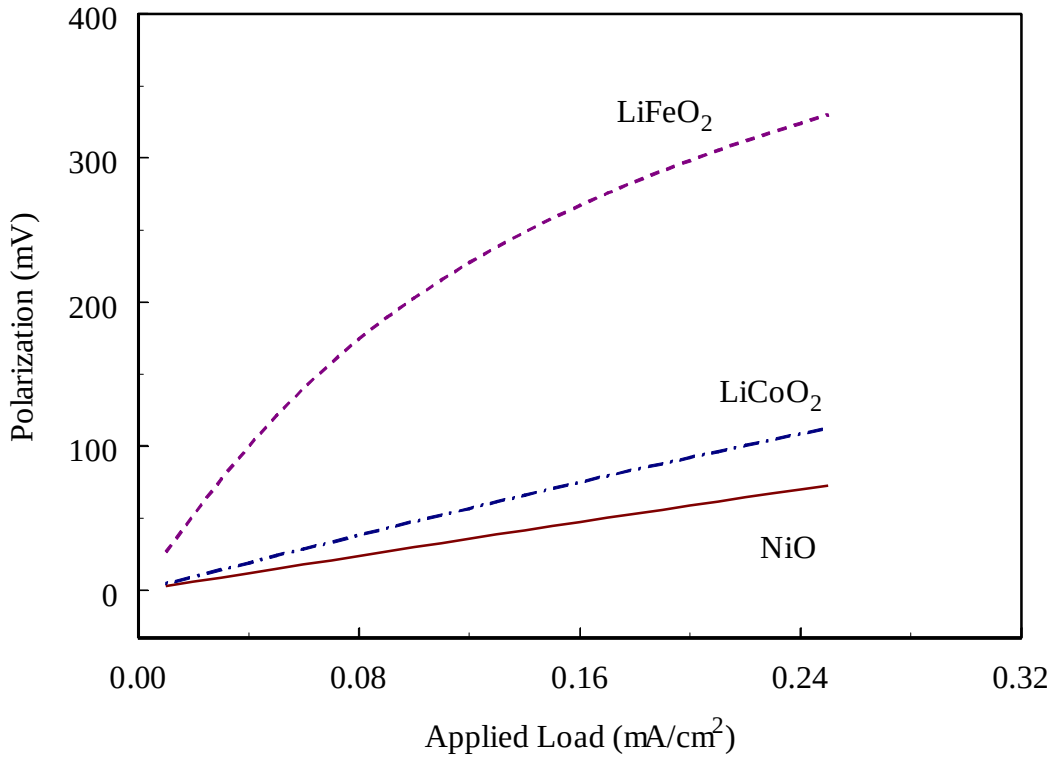

Figure 3. Cathode polarization curves simulated for different materials under various applied loads.

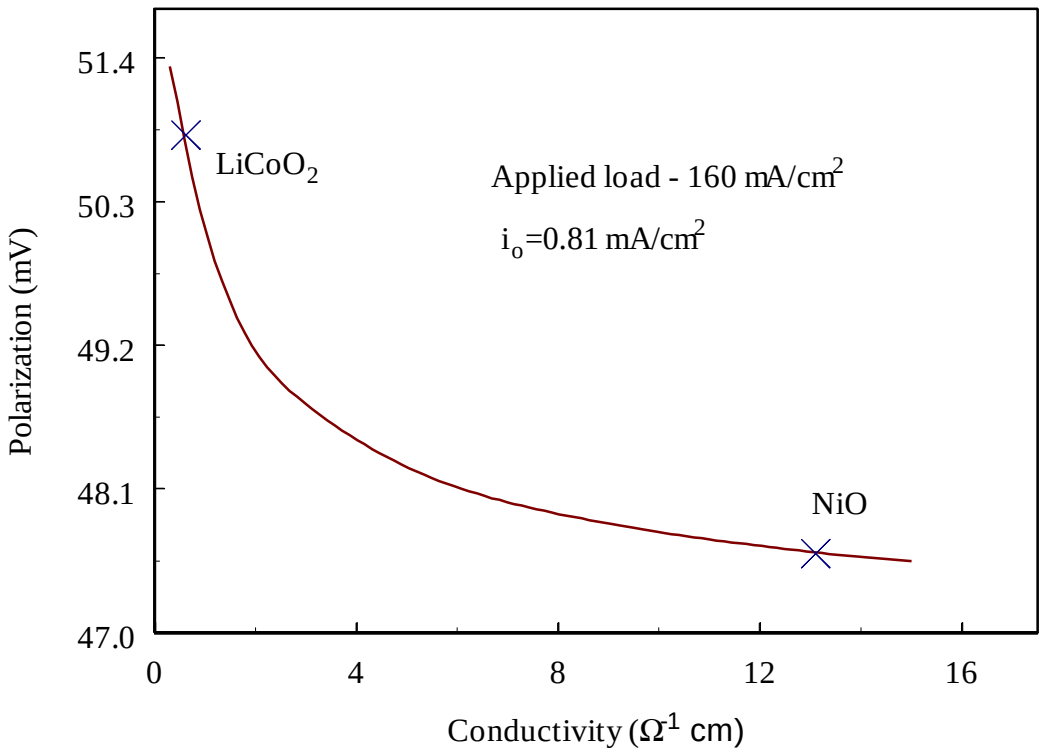

Figure 4. Change in cathode polarization as a function of electrode conductivity. We assume an exchange current density of 0.81 mA/cm^2 and an applied load of 160 mA/cm^2.

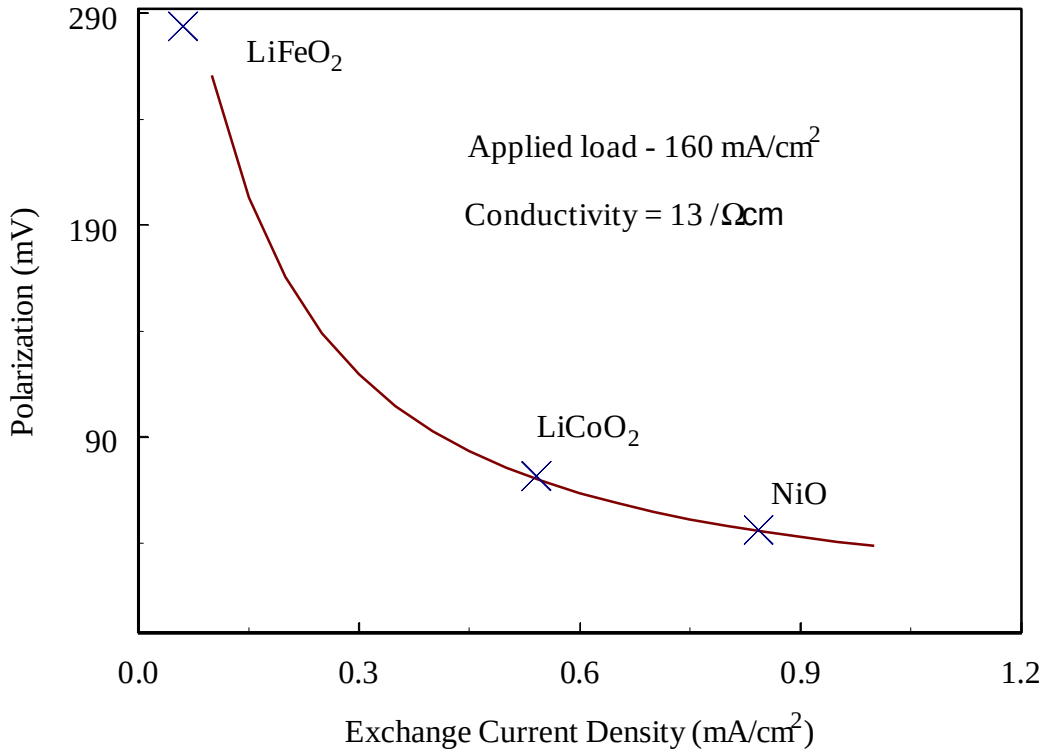

Figure 5. Cathode polarization plotted as a function of exchange current density. The electrode conductivity is13 $\Omega^{-1}cm^{-1}$ and the applied load is 160 mA/cm^2.

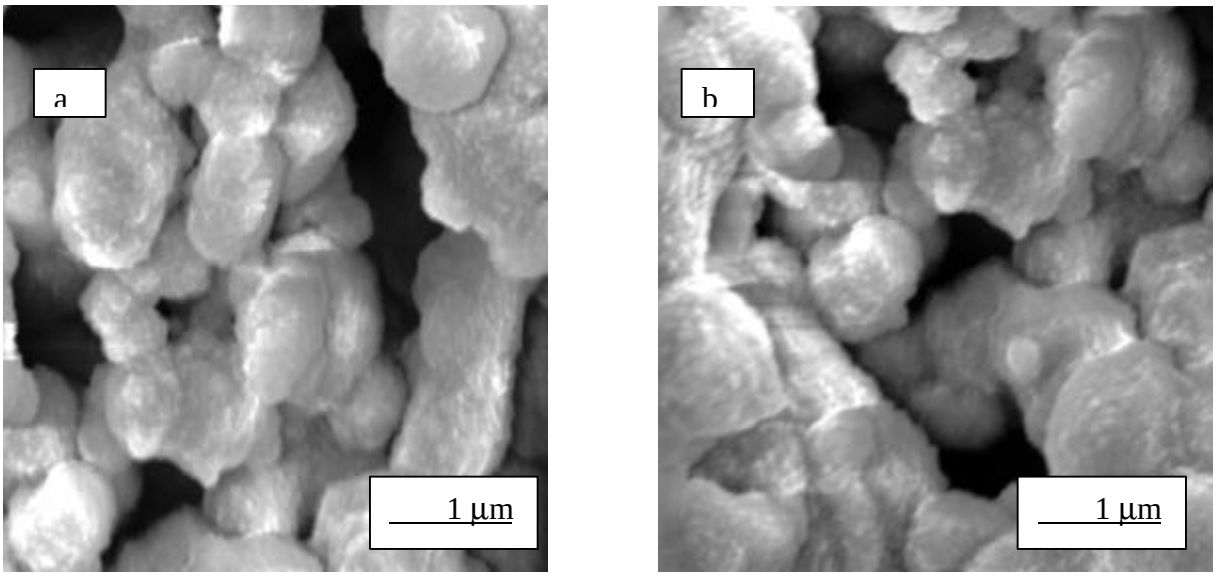

Figure 6. SEM photographs of bare (a, left) and cobalt microencapsulated (b, right) nickel electrodes obtained by tape casting and sintering.

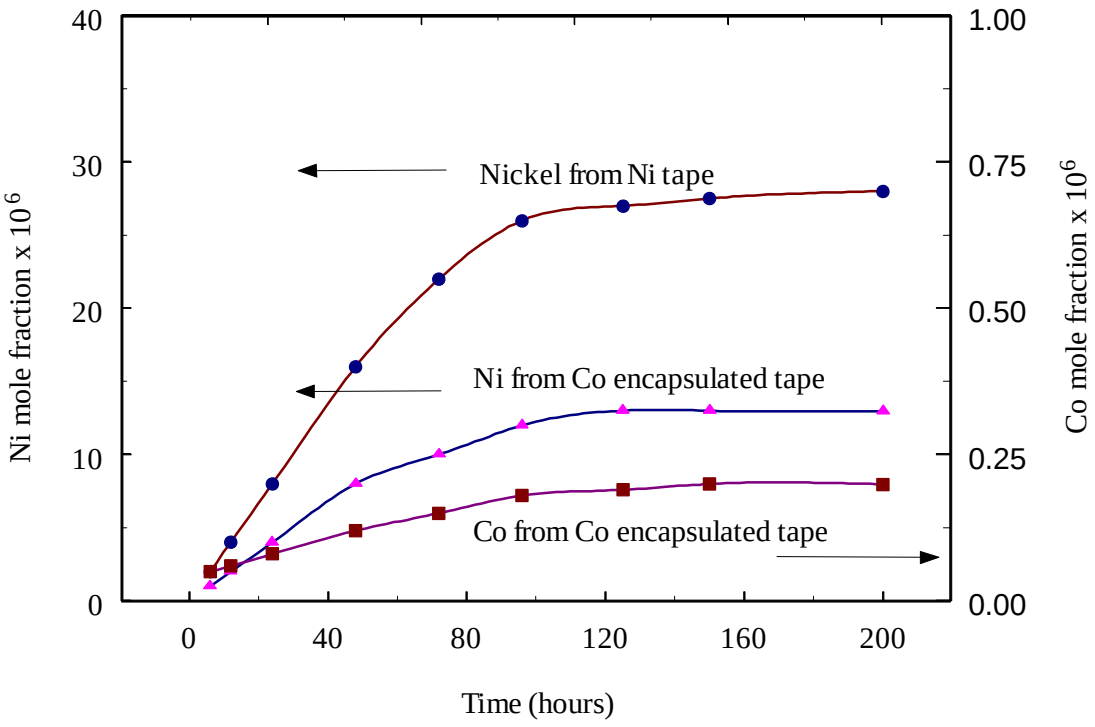

Figure 7. Atomic absorption spectroscopy analysis of dissolved nickel and cobalt in molten carbonate melt.

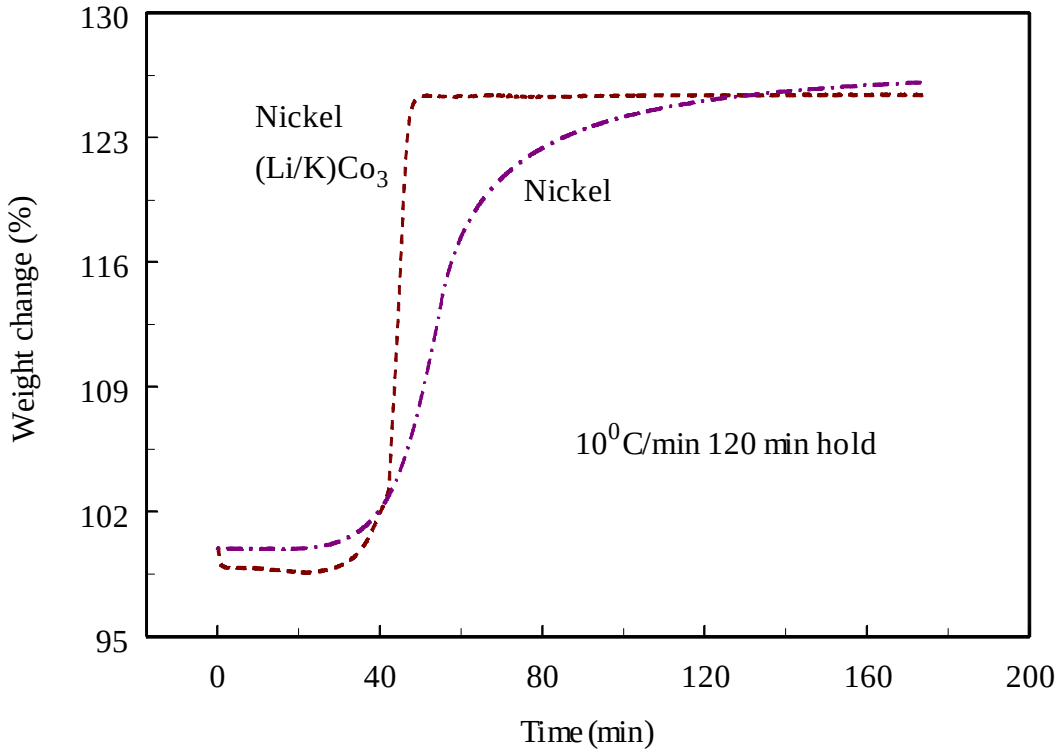

Figure 8a. TGA analysis of sintered nickel tape under cathode gas conditions in the presence and absence of molten carbonate melt.

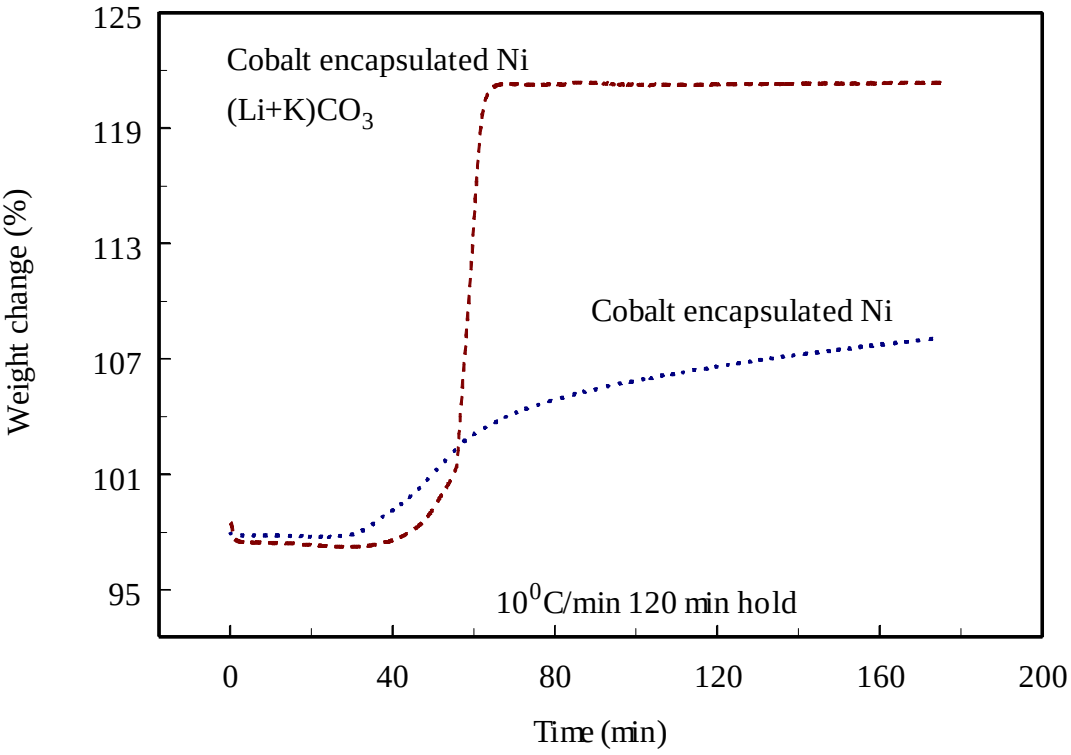

Figure 8b. TGA analysis of sintered cobalt encapsulated nickel tape under cathode gas conditions in the presence and absence of molten carbonate melt.

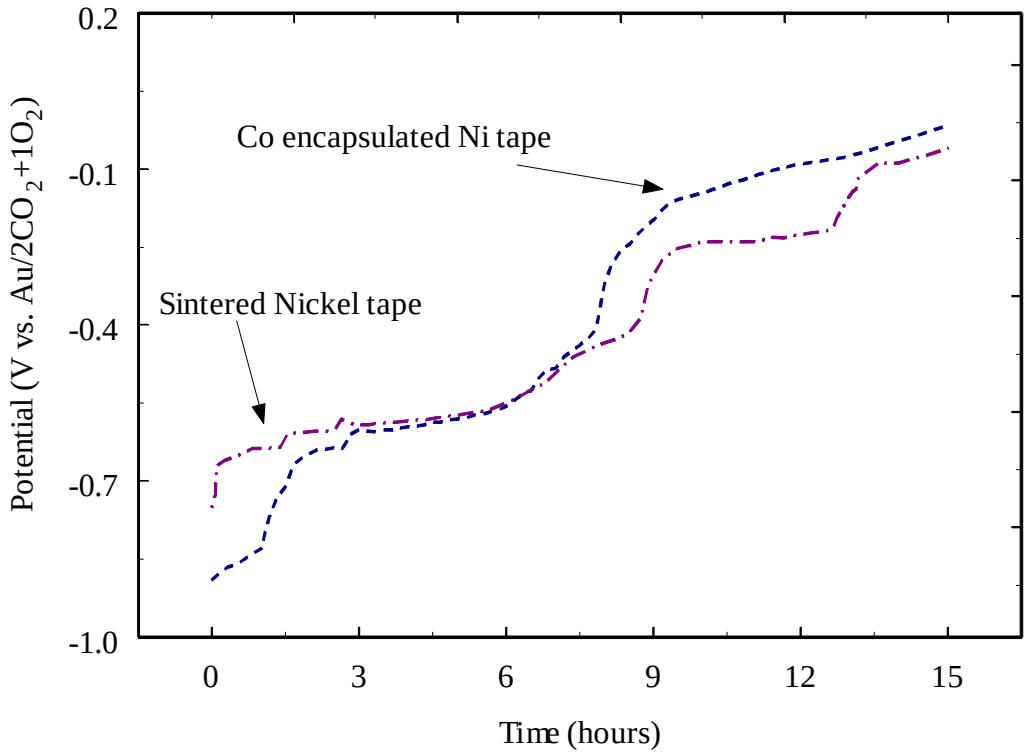

Figure 9. Open circuit potential as a function of time during the *in-situ* oxidation of bare and cobalt encapsulated nickel tapes under cathode gas conditions.

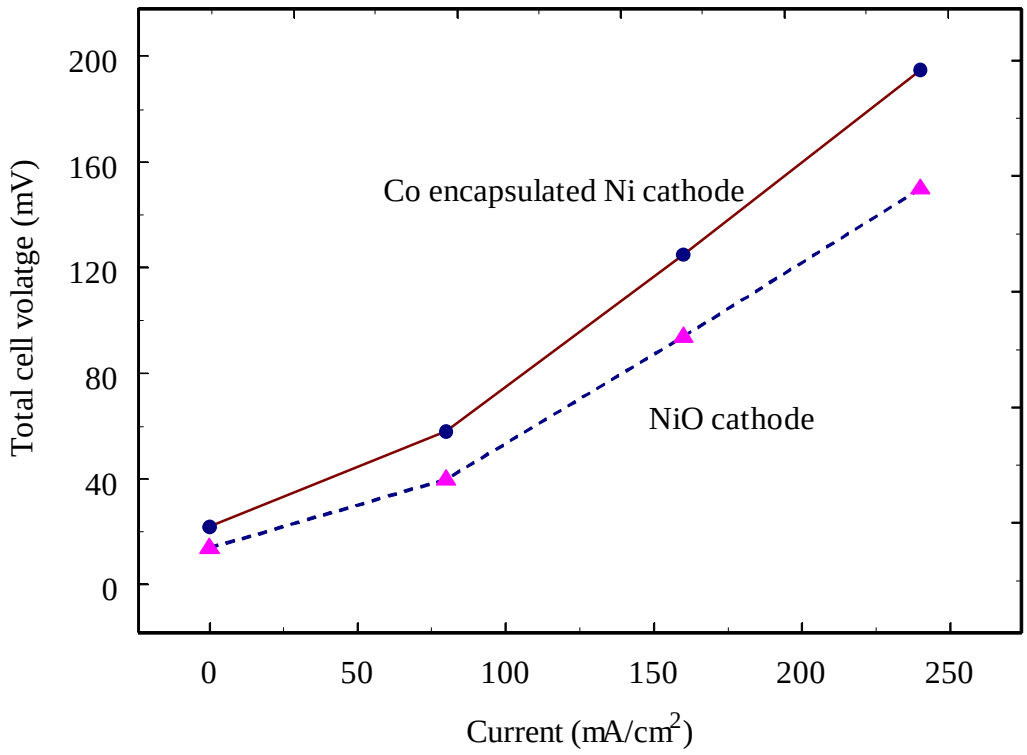

Figure 10. Comparison of cathode polarization behavior at different current loads for bare and cobalt encapsulated nickel cathodes.

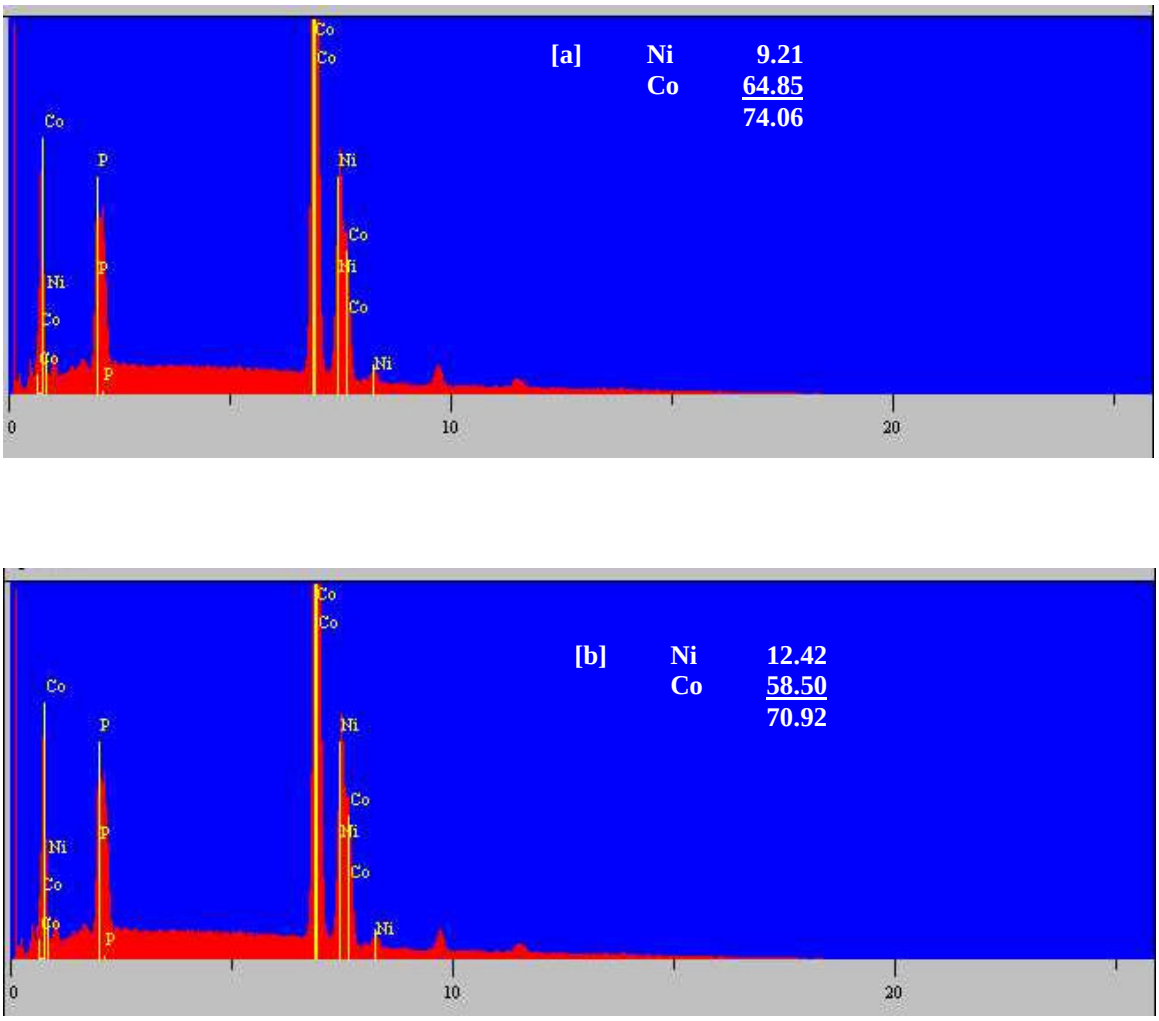

Figure 11. EDAX analysis done on cobalt encapsulated and bare nickel oxide cathodes after 72 hours (a) and 300 hours (b) of operation.

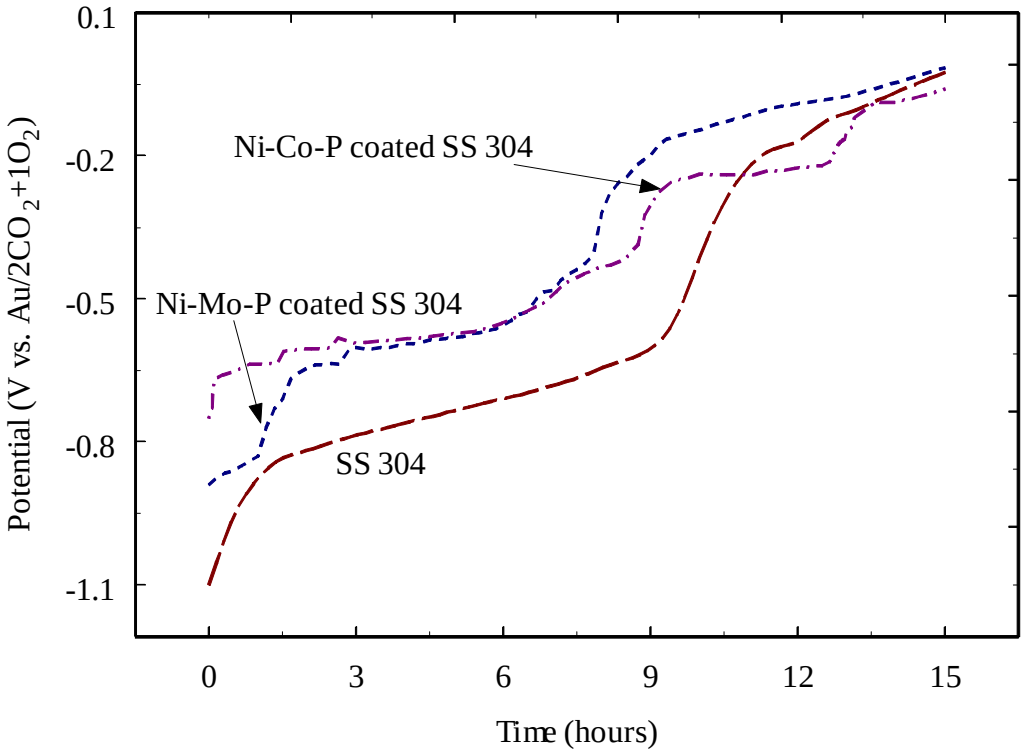

Figure 12. Open circuit potential response of bare and surface modified SS 304 as a function of exposure time in molten carbonate melt under cathode gas conditions. The potential is referenced to the oxygen reduction reaction happening on a gold electrode.

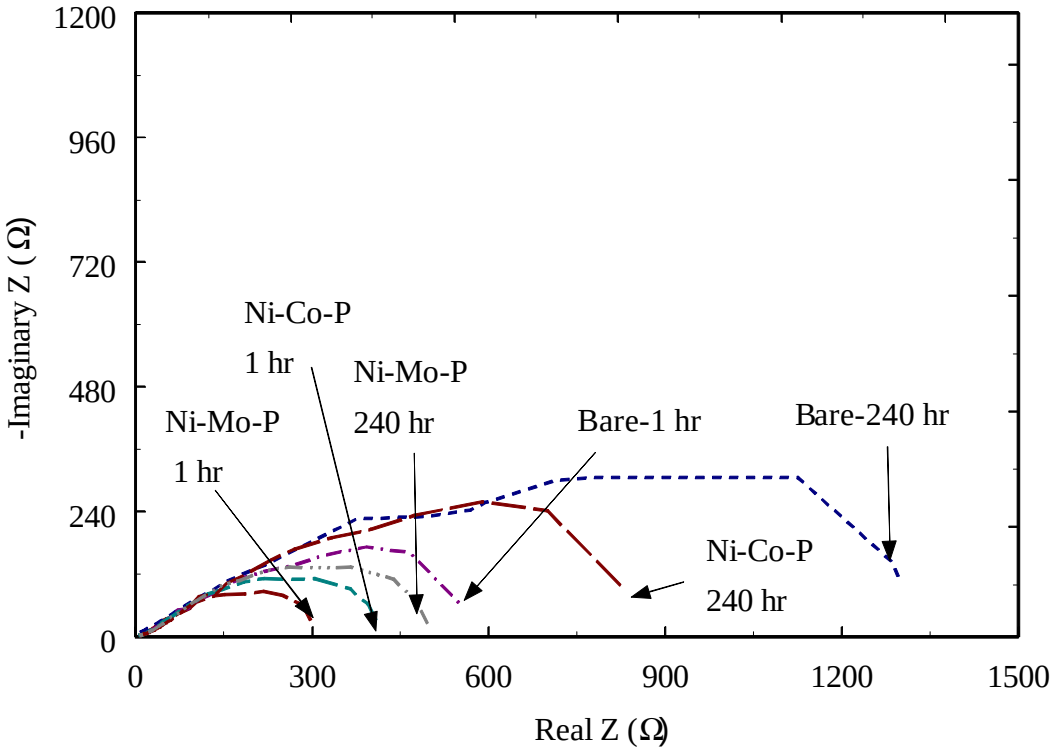

Figure 13. Nyquist plots of bare and surface modified SS 304 recorded after 1 hour and 10 days after immersion in molten carbonate melt under cathode gas conditions.